

Active Thrust on Retaining Wall – Point of Application and Distribution

D.M. Dewaikar* and S.A. Halkude†

Introduction

Coulomb's (1776) analysis of active thrust on retaining wall with cohesion-less backfill gives the magnitude of active thrust from force equilibrium considerations. The condition of moment equilibrium is not used in the analysis for the reason that distribution and point of application of reaction on the failure plane are not known.

One of the main deficiencies in Coulomb's theory is that, in general, it does not satisfy all static equilibrium conditions, since the three forces acting on the failure wedge generally do not meet at a common point, when failure is assumed to be along a plane surface.

If the point of application of reaction on the failure plane is known, point of application of active thrust can be calculated using moment equilibrium condition, so as to obtain a complete solution of the problem.

An analysis using Kötter's (1903, Terzaghi, 1943, Jumikis, 1969) equation is proposed here for obtaining the complete solution of retaining wall problem.

* Professor, Department of Civil Engineering, Indian Institute of Technology, Bombay, Mumbai, 400076, India Email: dmde@civil.iitb.ac.in

† Research Scholar, Department of Civil Engineering, Indian Institute of Technology, Bombay, Mumbai, 400076, India

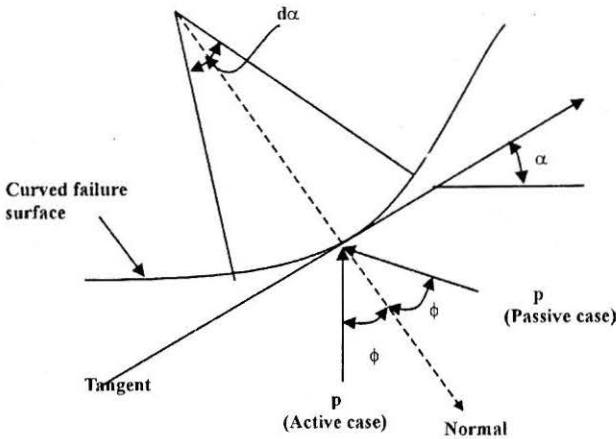


FIGURE 1 : Kötter's Equation for Curved Failure Surface

Analysis for Active Case

Kötter's Equation

This equation gives the distribution of reactive pressure on a curved failure surface, in a cohesion-less soil medium in active state of equilibrium, in the following form (Fig.1),

$$\frac{dp}{ds} - 2p \cdot \tan \phi \cdot \frac{d\alpha}{ds} = \gamma \sin(\alpha - \phi) \quad (1)$$

- in which,
- dp = differential reactive pressure on the failure surface
 - ds = differential length of arc of failure surface
 - ϕ = angle of soil internal friction
 - $d\alpha$ = differential angle
 - α = inclination of tangent at the point of interest with the horizontal and
 - γ = unit weight of soil

Distribution of Reactive Pressure on the Failure Plane

In Fig.2, a plane failure surface AB is shown as part of the failure wedge, ABC. The free body diagram of this wedge is also shown in the

same figure in which, the forces that are involved are, P_a the active thrust, W the weight of failure wedge, ABC and reaction, R on the failure plane, AB.

For a plane failure surface, $da/ds = 0$ and Eqn.1 takes the following form:

$$\frac{dp}{ds} = \gamma \cdot \sin(\alpha - \phi) \quad (2)$$

Integration of the above equation gives,

$$p = \gamma \cdot \sin(\alpha - \phi) \cdot s + C_1 \quad (3)$$

The above equation gives distribution of reaction, R in terms of corresponding pressure, p on the failure plane, AB and s represents the distance as measured from point B.

The constant, C_1 in Eqn.3 is evaluated from the boundary condition that pressure, p is zero at point, B, which corresponds to $s = 0$. With this condition, C_1 is zero and Eqn.3 becomes,

$$p = \gamma \cdot \sin(\alpha - \phi) \cdot s \quad (4)$$

Magnitude of Reaction on the Failure Plane

Using Eqn.4, the reaction, R is calculated as,

$$R = \int_0^{AB} p \cdot ds$$

Substitution for p from Eqn.4 into the above equation gives,

$$R = \int_0^{AB} \gamma \cdot \sin(\alpha - \phi) \cdot s \cdot ds$$

Integration yields,

$$R = \frac{1}{2} \cdot AB^2 \cdot \gamma \cdot \sin(\alpha - \phi) \quad (5)$$

In the above equation, r represents the distance of point of application of R (Fig.2) from the base, A of the wall.

With substitution for p from Eqn.4, the above equation becomes,

$$R \cdot r = \int_0^{AB} \gamma \cdot \sin(\alpha - \phi) \cdot s \cdot (AB - s) \cdot ds$$

$$\text{or, } R \cdot r = \gamma \cdot \sin(\alpha - \phi) \cdot \int_0^{AB} (AB \cdot s - s^2) \cdot ds$$

Integration yields,

$$R \cdot r = \gamma \cdot \sin(\alpha - \phi) \cdot \frac{AB^3}{6}$$

Substitution for R from Eqn.5 in the above equation gives,

$$\frac{1}{2} \cdot AB^2 \cdot \gamma \cdot \sin(\alpha - \phi) = \gamma \cdot \sin(\alpha - \phi) \cdot \frac{AB^3}{6}$$

from which,

$$r = \frac{1}{3} \cdot AB \tag{9}$$

where, the value of AB is as given by Eqn.6.

Magnitude of Active Thrust P_a

Referring to Fig.2, the following two force equilibrium equations are obtained:

Horizontal force equilibrium

$$P_a \cdot \sin(\theta - \delta) = R \cdot \sin(\alpha - \phi) \tag{10}$$

where δ is the angle of wall friction.

From the above equation, P_a is obtained as,

$$P_a = R \cdot \frac{\sin(\alpha - \phi)}{\sin(\theta - \delta)} \quad (11)$$

Vertical force equilibrium

$$P_a \cos(\theta - \delta) = W - R \cdot \cos(\alpha - \phi) \quad (12)$$

where W represents self-weight of the wedge, ABC.

From the above equation, P_a is obtained as,

$$P_a = \frac{W - R \cdot \cos(\alpha - \phi)}{\cos(\theta - \delta)} \quad (13)$$

It may be noted that both Eqns.11 and 13 give the magnitude of unknown thrust, P_a . These two equations will yield the same and unique value of P_a only when the equilibrium conditions correspond to those at failure, which are uniquely defined by a characteristic value of α , which can be determined by trial and error procedure.

Trial and Error Procedure

In this procedure, first a trial value of α (Fig.2) is assumed and corresponding weight, W of trial failure wedge, ABC is computed. Using Eqn.7, magnitude of R is computed and from Eqns.11 and 13, values of P_a are determined. If the trial value of α is equal to its characteristic value corresponding to the failure condition, the two computed values of P_a will be the same and otherwise, they will be different. For various trial values of α , computations are carried out till the convergence is reached to a specified (third) decimal accuracy.

Thus, in this method of analysis, failure plane is identified in such a manner that, force equilibrium of failure wedge; ABC (Fig.2) is satisfied. This approach is different from Coulomb's analysis in which, P_a is obtained from the considerations of its maximum value, i.e., α is identified in such a manner that maximum value of P_a is obtained from force equilibrium considerations.

The computed value of P_a was found to be exactly matching with the one, obtained from Coulomb's analysis.

Point of Application of Active Thrust

Moment equilibrium condition is now used to compute the point of application of active thrust. Equating moment of forces and reactions about point A (Fig.2), gives the following equation,

$$P_a \cdot \cos \delta \cdot x_1 = R \cdot \cos \phi \cdot r - W \cdot x_2$$

in which, the distances x_1 , x_2 and r are as shown in above referred figure.

From the above equation, x_1 is obtained as,

$$x_1 = (R \cdot \cos \phi \cdot r - W \cdot x_2) / P_a \cdot \cos \delta \quad (14)$$

The height, h of point of application of P_a from the wall base (Fig.2) is then calculated as,

$$h = x_1 \cdot \sin \theta \quad (15)$$

Computation of Earth Pressure Distribution on the Retaining Wall

Outline of the Proposed Method

The distribution of active earth pressure, p_n for the case of vertical wall is computed corresponding to the normal thrust, which is given as,

$$P_n = P_a \cdot \cos \delta \quad (16)$$

Referring to Fig.3, the normal active earth pressure, p_n at a point, which is located at a distance, z below the wall top can be expressed as,

$$p_n = a \cdot z^b \quad (17)$$

in which, a and b are the constants to be determined from the known boundary conditions.

The total normal active thrust P_n is then obtained as,

$$P_n = a \int_0^H z^b dz$$

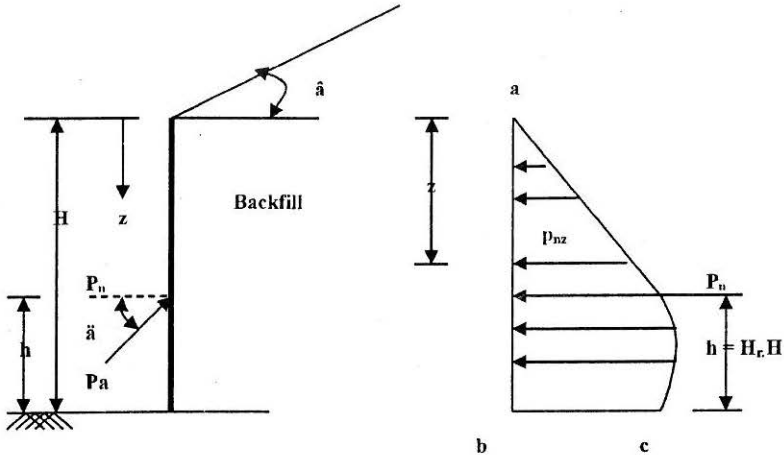


FIGURE 3 : Distribution of Normal Earth Pressure on the Vertical Retaining Wall

$$\text{or, } P_n = a \left[\frac{H^{b+1}}{b+1} \right] \quad (18)$$

The moment, M_1 of pressure distribution with respect to the base of wall is given as,

$$M_1 = \int_0^H p_n (H-z) dz = \int_0^H a \cdot z^b (H-z) dz$$

$$\text{or, } M_1 = \frac{a \cdot H^{b+2}}{(b+1)(b+2)} \quad (19)$$

The moment, M_2 of active thrust, P_n with respect to base of the wall is given as,

$$M_2 = H_r \cdot H \cdot P_n \quad (20)$$

where, H_r is the ratio of height of point of application of the thrust, with respect to wall height, H .

The moments, M_1 and M_2 should be equal, so that,

$$\frac{a \cdot H^{b+2}}{(b+1)(b+2)} = H_r \cdot H \cdot P_n \quad (21)$$

Substituting the value of P_n from Eqn.18 into Eqn.21, the constant, b is evaluated as,

$$b = \frac{H(1-2H_r)}{H \cdot H_r} = \frac{(1-2H_r)}{H_r} \quad (22)$$

By substituting the above value of b in Eqn.18, a is evaluated as,

$$a = \frac{(b+1) \cdot P_n}{H^{b+1}} \quad (23)$$

Therefore, the normal pressure distribution on the retaining wall is finally obtained as,

$$p_n = \frac{(b+1) \cdot P_n}{H^{b+1}} \cdot z^b \quad (24)$$

in which, b is as calculated from Eqn.22

Discussions

The basic purpose of this analysis was to compute the location of point of application of active thrust and study its variation with respect to several parameters that are involved in the analysis.

It was found convenient to express h in terms of its ratio with respect to H , in non-dimensional form (h/H). From the analysis, it was found that this ratio (H_r) varied over a wide range, with combinations of several parameters such as angle of wall back, angle of backfill slope, angle of wall friction and angle of soil internal friction. A vast multitude of data was obtained and a few important results are discussed here.

Active Thrust

The effect of various parameters on the location of point of application of active thrust is discussed below separately.

Angle of wall back

In Fig.4, variation of H_r with angle of wall back, θ is shown for δ and β of 4° each. It is seen that H_r varies in the range of 0.33 to 0.49. It decreases with increasing θ , with higher values for higher ϕ .

As seen from the figure, for the case of a vertical wall with backfill slope angle and wall friction angle being the same, which corresponds to Rankine's case, in which, the direction of thrust is parallel to the backfill slope; H_r has a unique value 0.333, for all values of ϕ .

In Fig.5, the variation of H_r with angle of wall back, θ is shown for δ and β of 8° and 0° respectively. It is seen that, H_r varies in the range of 0.30 to 0.47. With increasing θ , it decreases, with higher values for higher ϕ .

Angle of wall friction

In Fig.6, variation of H_r with δ is shown for θ and β of 85° and 0° respectively. It is seen that H_r varies in the range of 0.23 to 0.39. It decreases with increasing δ , with higher values for higher ϕ .

Angle of backfill slope

In Fig.7, variation of H_r with β is shown, for θ and δ of 80° and 8° respectively. It is seen that H_r varies in the range of 0.35 to 0.45. It increases with increasing β , with higher values for higher ϕ .

Active Pressure Distribution on Retaining Wall

Referring to Fig.3, the location of point, which is at a distance, z below the wall top is expressed in terms of its ratio with respect to height of wall, H in non-dimensional form (z/H) . Corresponding normal earth pressure, p_n at the point is expressed in non dimensional form as $(p_n/\gamma \cdot H)$.

Computations are made for the case of a vertical retaining wall. The effect of parameters such as β , δ and ϕ on normal earth pressure distribution is discussed below separately.

Angle of wall friction

Figure 8 shows variation of normal earth pressure with angle of wall friction, for angles of soil internal friction and backfill slope of 25° and 0° respectively. The distribution is linear for $\delta = 0^\circ$ and with increasing values of δ , it tends to be more nonlinear. The magnitude of earth pressure decreases

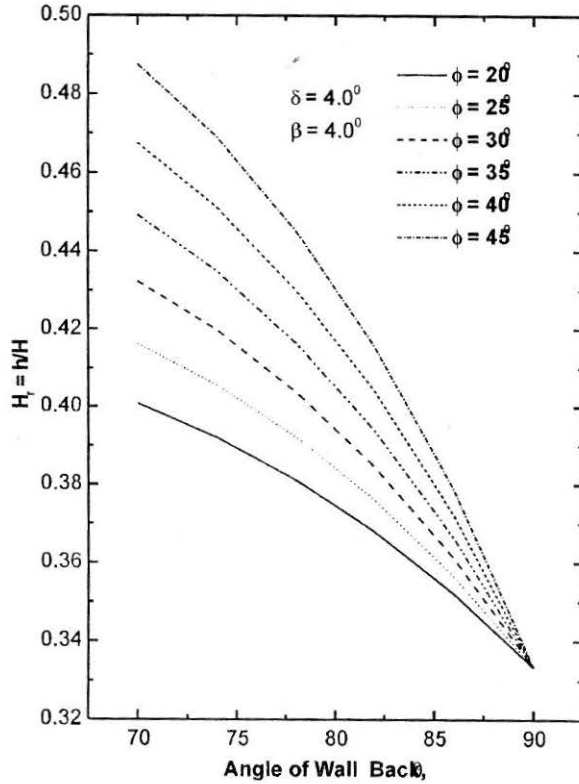


FIGURE 4 : Variation of H_r with Angle of Wall Back, θ

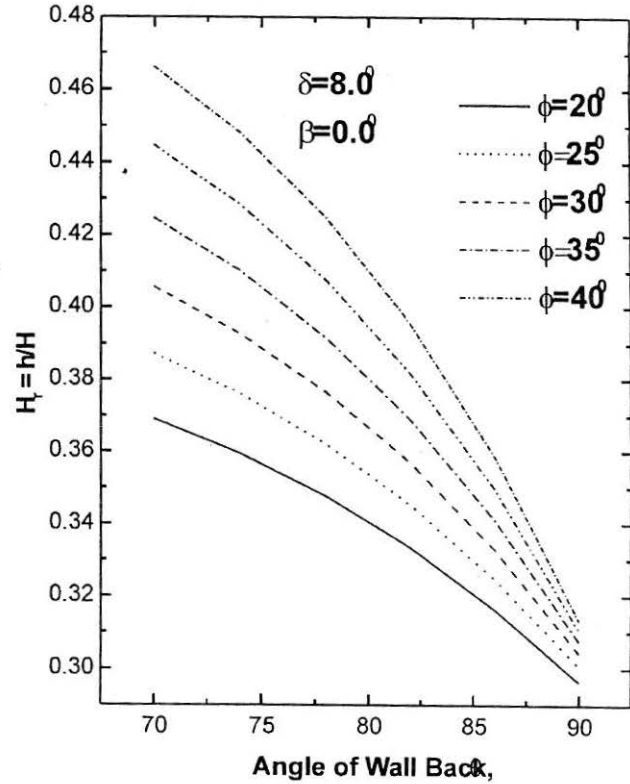


FIGURE 5 : Variation of H_r with Angle of Wall Back, θ

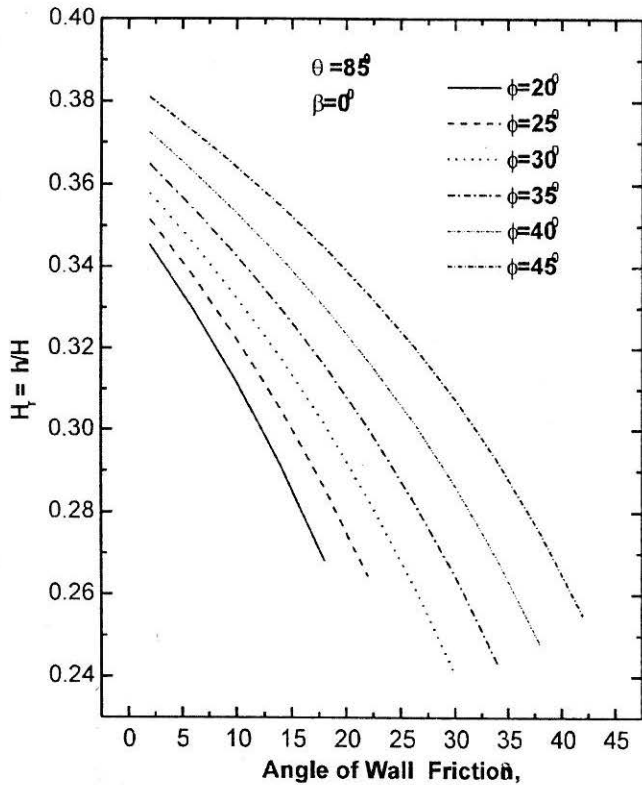


FIGURE 6 : Variation of H_r with Angle of Wall Friction, δ

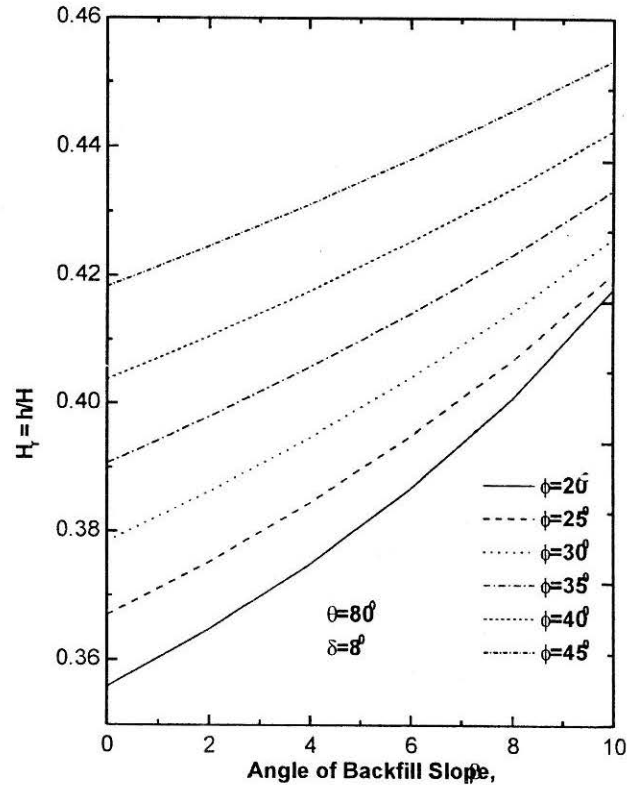


FIGURE 7 : Variation of H_r with Angle of Backfill Slope, β

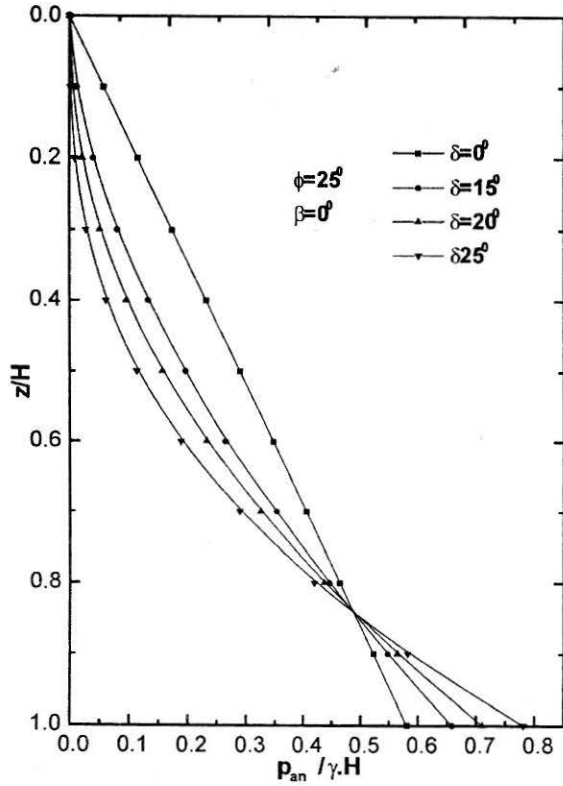


FIGURE 8 : Variation of Normal Active Pressure with Wall Friction, δ

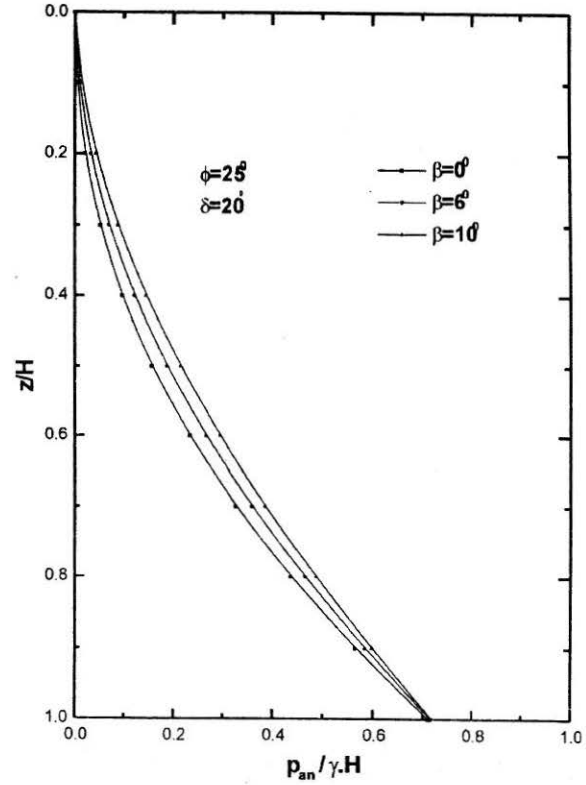


FIGURE 9 : Variation of Normal Active Pressure with Angle of Backfill Slope, β

with increasing δ upto a characteristic non-dimensional depth z/H , beyond which, a reverse trend is observed.

Angle of backfill slope

Figure 9 shows variation of normal earth pressure for angles of soil internal friction and wall friction of 25° and 20° respectively. The distribution is nonlinear and with increasing β , it tends to be more nonlinear. The magnitude of earth pressure increases with increasing β and it is interesting to note that all the curves converge at a point at the wall base. This means that, maximum value of the normal earth pressure is not affected by the backfill slope.

Angle of soil internal friction

Figure 10 shows variation of normal earth pressure for angles of wall friction and backfill slope of 10° and 0° respectively. The distribution is nonlinear and with increasing ϕ , it tends to be linear. The magnitude of earth pressure is higher for lower values of ϕ .

Comparison with experimental results

Experimental results reported by Fang and Ishibashi (1986) for the case of a vertical wall retaining horizontal cohesion-less backfill are shown in Fig.11, for rotation of wall about its base. Using the same data, normal earth pressure distribution has been computed and is reported in the same figure. It is seen that, there is a reasonably good agreement between the results of proposed analysis and experimental results. The trends indicated by both the results are similar, with nonlinear nature of the distribution.

It may also be noted here that, one of the assumptions in Coulomb's theory is that, active conditions develop with the rotation of wall about its base (Terzaghi, 1941 and Bang, 1985).

Conclusions

Complete solution to retaining wall problem is obtained only when the distribution and location of point of application of reaction on the failure plane are known. Kötter's equation lends itself as an effective tool in the proposed analysis. The method of analysis identifies the failure plane from the consideration of force equilibrium. Moment equilibrium equation is used to compute the point of application of the active thrust.

One of the main deficiencies in Coulomb's theory is that, the three forces (weight of failure wedge, soil reaction and earth thrust) acting on the

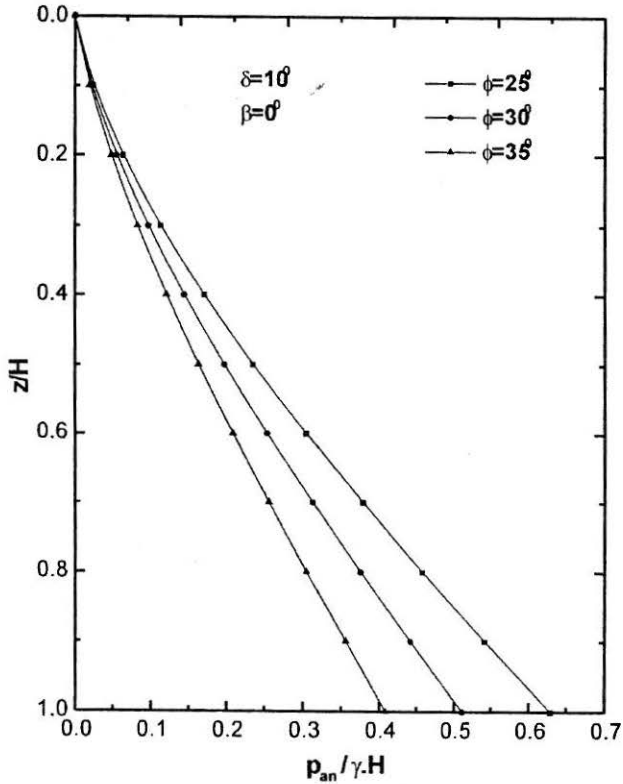


FIGURE 10 : Variation of Normal Active Pressure with Angle of Soil Internal Friction, ϕ

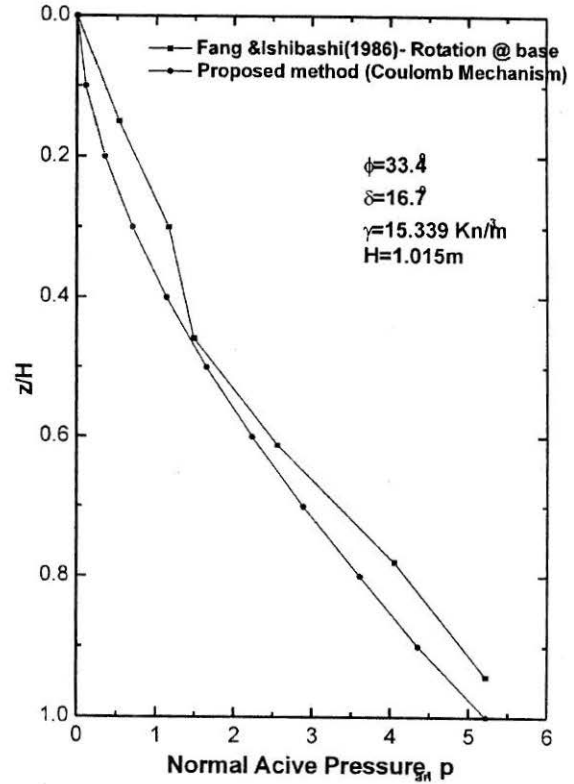


FIGURE 11 : Comparative Normal Active Pressure Distribution Curves

failure wedge generally do not meet at a point, thus, not complying with moment equilibrium. This is rectified in the proposed analysis, since all the conditions of static equilibrium are used effectively.

The analysis clearly shows that location of point of application of active thrust depends upon combinations of several parameters such as angles of soil internal friction, wall friction, wall back and backfill slope.

Reasonably good agreement is observed between the results of proposed active pressure distribution analysis and available experimental results in respect of wall rotation about its base. The trends indicated by both the results are similar, with non-linear nature of distribution.

References

- BANG, S. (1985) : "Active Earth Pressure Behind Retaining Walls", *J. Geotech. Engg.*, ASCE, 3, pp.407-412.
- FANG, Y.S. and ISHIBASHI, I. (1986) : "Static Earth Pressure with Various Wall Movements", *J. Geotech. Engg.* ASCE, 112(3), pp.317-333.
- JUMIKIS, A.R. (1962) : *Soil Mechanics*, Von Nostrand Reinhold Co.
- JUMIKIS, A.R. (1969) : *Theoretical Soil Mechanics*, Von Nostrand Reinhold Co.
- TERZAGHI, K. (1941) : "General Wedge Theory of Earth Pressure", *Transactions: ASCE*, pp.68-80.
- TERZAGHI, K. (1943) : *Theoretical Soil Mechanics*, John Wiley and Sons, Inc., New York.